Scientific Research Publishing

Computational Chemistry, 2022, 10, 97-119
https://www.scirp.org/journal/cc
ISSN Online: 2332-5984
ISSN Print: 2332-5968

The Oryzenin's Effect on Di, Tri and Quadri-Saccharide Degradation. An Investigation by a Mixed Method: ONIOM (DFT/B3LYP/6 - 31 + G(d, p): AM1)

N'guessan Boka Robert, Bamba El Hadji Sawaliho*, Koffi Kouassi Alain

Laboratoire de Constitution et de Réaction de la Matière, UFR SSMT, Université Félix Houphouët-Boigny, Abidjan, Côte d'Ivoire
Email: *bambaelhadjisawaliho@yaoo.ca

How to cite this paper: Robert, N.B., Sawaliho, B.E.H. and Alain, K.K. (2022) The Oryzenin's Effect on Di, Tri and Quadri-Saccharide Degradation. An Investigation by a Mixed Method: ONIOM (DFT/B3LYP/6 - 31 + G(d, p): AM1). *Computational Chemistry*, **10**, 97-119.
https://doi.org/10.4236/cc.2022.102005

Received: January 4, 2022
Accepted: April 26, 2022
Published: April 29, 2022

Abstract

The paddy rice degradation remains a concern for research; the chemical phenomena underlying this process persists unknown. This research aims to identify the mechanism of starch degradation. It determines the nature of the reactions between two, three and four synthons of amylose with oryzenin using theoretical methods. The ONIOM (DFT/B3LYP/6 - 31 + G(d, p): AM1) level of theory is performed on four monomers and eight complexes. Frequencies make it possible to obtain energy and spectroscopic quantities. Calculations after geometry optimization. Following this, a "single point" allows exploiting the "Natural Bond Orbital (NBO)" analysis. The first three parameters suggest that the main interactions between oryzenin and amylose arise through O_{29}-H_{30}…O_{46} hydrogen bonds (HB). Furthermore, this result posits that the length of the amylose doesn't influence this reaction. The NBO analysis shows that this component of starch degrades first at the end of the chain to produce monosaccharides; it can also alter in the middle of the chain to give disaccharides.

Keywords

Paddy Rice, Oryzenin, Amyloidosis, Hydrogen Bond

1. Introduction

The article is part of the fight against food shortages. It's interesting in the factors likely to limit them [1]. It focuses on those potentially linked to rice post-harvest losses. It aims to contribute to the debate on the renovation of rice production or conservation methods. The latter remains a highly strategic, but poorly perform-

ing sectors [2].

According to [3], rice growing reduced the available irrigated areas by 4 to 5 million hectares per year since the 1970s. At the same time, yields have stagnated after 1966. These have reached 30% worldwide. For [2] and 24% in West Africa [4]. According to [3], the sector contributes to water pollution and the risk of disease; it uses pesticides extensively. Intensive irrigation promotes salinization and waterlogging of the soil. submersion is a major source of methane emissions Nitrogen fertilizers have created greenhouse gases that cause global warming. Debates suggest finding environmentally friendly ways to produce abundantly and healthily or efficiently conserve rice; its demand continues to grow at the start of the 21st century [4]. The challenge for the sector is to produce enough rice while sparing natural resources and reducing post-harvest losses. These refer to the spoiled quantities between its harvest and its transformation into food products [4].

Biotechnology offers solutions through various varieties of hybrid rice. According to [5] it transfers gene fragments from other plants or organisms to landraces or primary plant material. It's based on genomic and transformation techniques that have been in place for more than twenty years.

Moreover, available hybrid rice receives yields and nutritional quality [4]. They rarely incorporate a device that delays its degradation. This work proposes to highlight information likely to preserve it durably. It plans to elucidate the molecular dynamics underlying the harmful activity of its oryzenin. It wants to specify the mechanisms by which the latter deteriorates its starch.

Starch represents 90% of rice dry weight [6]. Its storage appears part of its preservation strategy [7]. However, storage over long periods leads to a change in its physical properties. It transforms its structure. It modifies its chemical and biological parameters, rice losses organoleptic characteristics and nutritional values. Many storage techniques remain being experimented to deal with this problem [8] [9]. These include the use of chemicals [10], phosphine gas fumigation [11], low temperature and inert atmosphere storage [12]. All these solutions stay ineffective; post-harvest losses persist significantly. Several factors cause its deterioration.

Starch deterioration goes related to temperature and humidity [13]. This work conjectures that its degradation is explained chemical interactions between its components; specifically, this process concerns those between its starch amylose or the amylopectin and its oryzenin [14] [15]. The literature doesn't provide any mechanism to justify this reaction. This work directs to fill this gap through the following question:

Through what mechanism does oryzenin degrade amylose in rice starch?

This exploratory research focuses on amyloidosis. It aims to determine the mode of amylose cleavage. It targets to establish its alteration mechanism. It has vital challenges; the degradation mechanism of this strategic foodstuff is poorly documented. The theoretical study of the amylose-oryzenin supramolecular stays unknown. It argues that the formation of HB between the two molecules explains

the degradation of the first. These affect the stability of several essential molecular structures such as water or DNA [16] [17]. They play a key role in a lot of areas of chemistry, physics, and biology [18] [19] [20]. This research exploits theoretical chemistry resources to answer the research question.

Many works describe HB in terms of charge transfer [21] [22] [23]. They discuss it by employing the Natural Bond Orbital (NBO) analysis [24]. This research involves this theory to elucidate HB of the supramolecular. It's based on interactive ones to analyze them. These reveal the interaction sites between two (AM2G), three (AM3G) or four (AM4G) amylose subunits and oryzenin. These theoretical and methodological approaches establish that oryzenin degrade starch by using the hydrogen bond between the oxygen of the osidic bridge (bridges) and its electrophilic site H_{30}. This mechanism explains the abundance of monosaccharides and disaccharides, to a lesser extent, in the starch degradation products of rice. The article contains two parts.

The first describes the materials and methods. It portrays the computational techniques. It presents the electrostatic potential (ESP), geometric, energetic, and spectroscopic quantities. It also examines NBO analysis. The second section discusses the results. The following section expounds on the materials and computational methods.

2. Materials and Calculation Methods

The ONIOM (Own N-layered Integrated molecular Orbital and Molecular mechanics) method allows the study of large systems [25] [26]. It provides a substantial advantage in terms of calculation time because it partitions the study system into several layers. Different levels of accuracy live used. The amylose-oryzenin complex is divided in two layers. The inside part corresponds to the environment where oryzenin interacts with the oxygen of the osidic bridge. The DFT/B3LYP/6 - 31 + G(d, p) theory deals with it. The rest of the amylose-oryzenin system stand carried out by the semi-empirical method AM1 calculation, which appears less accurate.

The complex and the various fragments are optimized using the Gaussian 09 software [27]. The nature of these structures was assessed through a frequency. Subsequently, a single point at the same level of theory offers the opportunity to perform NBO calculation [28].

The interactions are those established between osidic bridge's oxygen of amylose (through its subunits) and the donor hydrogen of oryzenin. The atoms live numbered as automatically generated by the Gauss view 06 software. However, for AM4G, the numbers 1 and 2 refer to the oxygen of the terminal and midchain osidic bridge respectively as shown in **Figure 1**. A red ball labels an oxygen atom. A big white corresponds to a carbon. A small schematizes hydrogen.

2.1. Electrostatic Potential

The electrostatic potential (ESP) stands an effective descriptor for determining

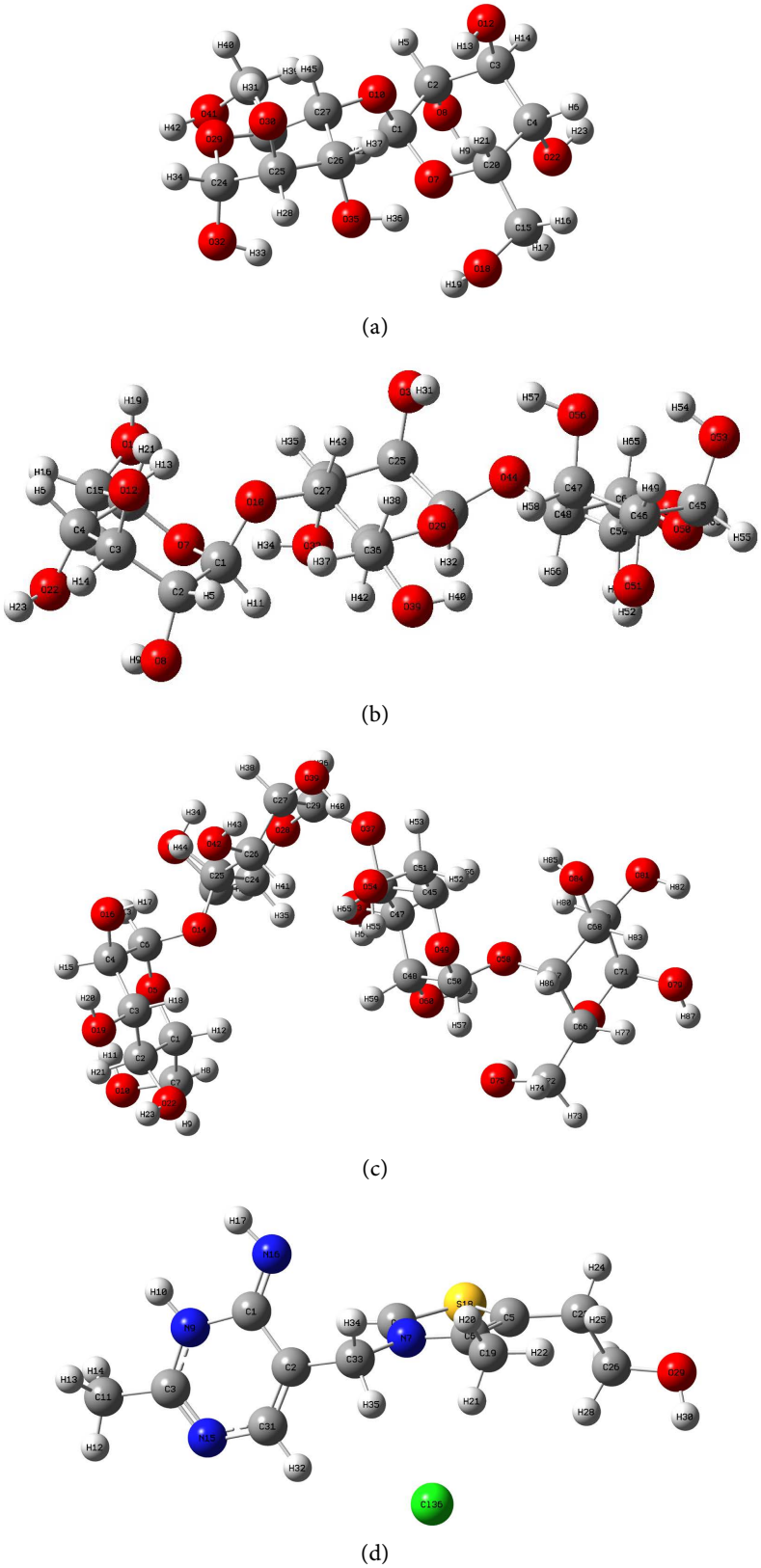

(a)

(b)

(c)

(d)

Figure 1. 3D structures of AM2G, AM3G, AM4G and ORYZENIN. (a) 3D structures of AM2G; (b) 3D structures of AM3G; (c) 3D structures of AM4G; (d) 3D structures of ORYZENIN.

preferential sites for electrophilic or nucleophilic attack. It helps to identify HB in organic compounds [29] [30] [31]. Equation (2-2) suggests that this statistic concern the interaction energy V, on the one hand, between a proton and those of the nucleus and, on the other hand, with the electrons of a molecule:

$$V(r)=\sum_{A}^{\text{Nucleus}}\frac{Z_A}{|R_A-r|}-\int\frac{\rho(r')\mathrm{d}r'}{|r'-r|} \tag{2-2}$$

Z_A is the charge of the nuclei A. R_A-r and $r'-r$ are corresponding to the proton-nucleus and proton-electron distances respectively. $\rho(r')$ is the electronic density. The first term represents the repulsion energy between nuclei and protons. The second reflects that relating to the attraction between them and the electrons. Furthermore, in regions where the influence of the latter dominates, the sign of $V(r)$ becomes negative. These sites are around free pairs of heteroatoms. An HB donor will be attracted to the point where $V(r)$ has its lowest $V_{\text{s,max}}$ value on the molecular surface. This latter corresponds to a surface of electronic "isodensity" [32].

Furthermore, the potential $V(r)$ becomes positive if the influence of the nucleus goes greater. It's also observed around atoms that behave like Lewis's acids. This study exploits the potential $V_{\text{s,max}}$ to identify sites favourable to oryzenin HB. These can have their geometric parameters.

2.2. Geometric Parameters of the Hydrogen Bond

HB stands an attractive interaction. The latter arise between the hydrogen of X-H within a molecule with one or more of their nucleophilic atoms. These are at the distance d [33] from the hydrogen. The first atom losses associated with oxygen or nitrogen of the molecule.

Here, it arises from the approach between the hydrogen of oryzenin with the osidic bridge's oxygen of amylose. Before the optimization of the complexes, the linearity angle α goes set to 180˚. The hybridization state of the last two atoms finds sp^3; β reports 109.5˚ (**Figure 2**). The distance d from oxygen to hydrogen remains identical to 2 Å. It corresponds to the minimum approach length of the two.

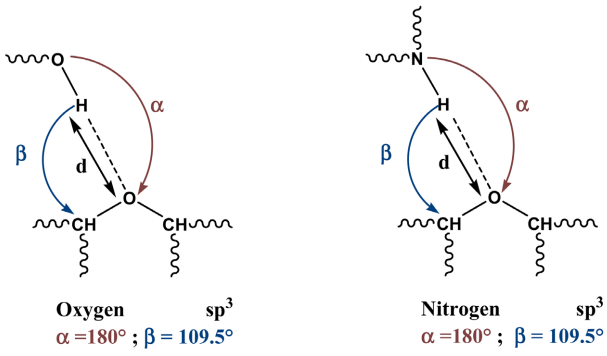

Figure 2. Angles of linearity α, directivity β and the minimum distance d describing the hydrogen bond.

According to [34], an HB can exist if d appears smaller than the sum of the Van der Waals radii of oxygen (1.52 Å) and hydrogen (1.1 Å) [35]. In other words, if $d \leq 2.62$ Å [36] [37], HB becomes strong if d decreases and if the angles α and β don't deviate too much from their ideal values. Moreover, its characterization attends clarified by the energy parameters.

2.3. Energy Parameters of Hydrogen Bond

HB formation brings about a change in enthalpy, free enthalpy, and entropy. These quantities correspond to the differences obtained between the complex form and the monomer of a molecular entity. For a reaction at 298.15 K, with the contributions of the translational, rotational, and vibrational entropy, the variation of these can be determined using Equations (2-3):

$$\Delta S_{298\mathrm{K}} = \sum S_{\mathrm{Complex}} - \sum S_{\mathrm{Monomers}} \tag{2-3}$$

Similarly, the free enthalpy or energy of the Gibbs reaction at 298.15 K is obtained from Equations (2-4). More, the present work uses spectroscopic descriptors to characterize HB.

$$\Delta G_{298\mathrm{K}} = \Delta H_{298\mathrm{K}} - T\Delta S_{298\mathrm{K}} \tag{2-4}$$

where:

$$\Delta H_{298\mathrm{K}} = \Delta E_{298\mathrm{K}} + \Delta nRT \tag{2-5}$$

2.4. Spectroscopic Descriptors of Hydrogen Bond

The formation of HB leads to a weakening of the X-H bond, it appears associated with its elongation and the simultaneous decrease of its stretching frequency. However, for many examples, this frequency increases with the contraction of the bond during the formation of the HB [38] [39]; spectroscopic descriptors represent an interesting tool to determine the strength of the HB. The relative displacement of H about X can be calculated using the following relationship:

$$\upsilon = \upsilon_{\mathrm{free}} - \upsilon_{\mathrm{complex}} \tag{2-6}$$

In practice, the higher the $\Delta\upsilon$ variation, the more HB formation is enabled. Moreover, NBO analysis permits verifying the formation process of HB.

2.5. NBO Analysis

NBO analysis appears a method to study donor-acceptor exchanges for intra- and intermolecular HB. It also permits the evaluation of charge transfer and conjugate interactions in chemical systems [40] [41]. It considers the important role of atoms free pairs in chemical processes. It allows accessing to the intermolecular energy of HB associated with the X-H…Y type. It evaluates the stabilization energy $E^{(2)}$ between the free doublet σ(Y) of the electron donor and the antibonding orbital σ^*(X-H) of the proton (electron acceptor) using the second-order perturbation theory. For each donor (i) and acceptor (j), the stabilization energy

$E^{(2)}$ connected with the delocalization $(i)\rightarrow(j)$ is estimated as follows:

$$E^{(2)} = \Delta E_{ij} = q_i \frac{F(i,j)}{\varepsilon_i \varepsilon_j} \tag{2-7}$$

where $F(i, j)$ stands a non-diagonal element of the Fock matrix, q_i represents the electron density in the donor orbital. ε_i and ε_j find the energies of the occupied (i) and vacant (j) NBO orbitals. The stabilization origin of a molecule comes from $E^{(2)}$. The higher this latter, the stronger the interaction is. However, this study only considers exchanges with an $E^{(2)}$ value above 1.5 kcal·mol^{-1}. The present work reveals the results of the calculations and discusses them.

3. Results and Discussion

This section first focuses on the ESP of the entire oryzenin surface. It reveals its main donor sites; these can likely to interact with amylose acceptors [42].

3.1. Electrostatic Potential: Sites of Molecular Interaction

Table 1 presents the $V_{s,max}$ of all hydrogen atoms in oryzenin. Figure 3 shows the map of its electrostatic potential. The values of $V_{s,max}$ varies from -2.9×10^3 kJ·mol^{-1} to -2.5×10^3 kJ·mol^{-1}. The largest appears those of H_{10} and H_{30} linked

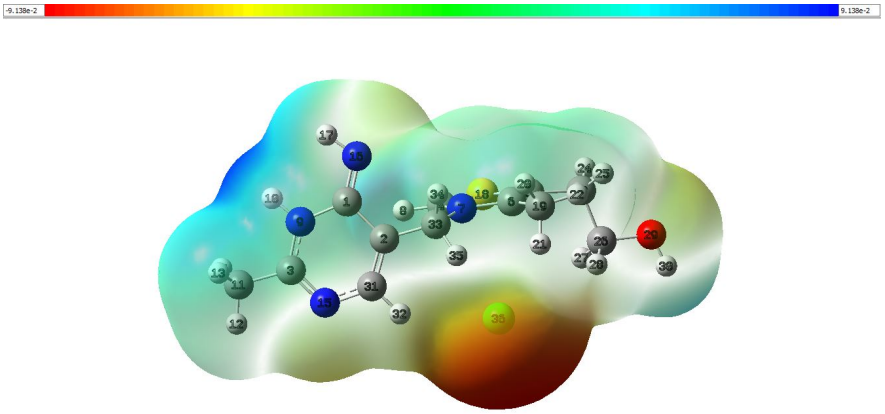

Figure 3. Aspect of oryzenin's electrostatic interaction potential map.

Table 1. Average electrostatic interaction potential V_s (in kJ·mol^{-1}) of different oryzenin donor sites.

Sites	$V_s * 10^3$ (kJ·mol^{-1})	*Sites*	$V_s * 10^3$ (kJ·mol^{-1})	*Sites*	$V_s * 10^3$ (kJ·mol^{-1})
C_7H_8	−2.7	$C_{19}H_{20}$	−2.9	$C_{26}H_{28}$	−2.9
N_9H_{10}	−2.5	$C_{19}H_{21}$	−2.9	$O_{29}H_{30}$	−2.6
$C_{11}H_{12}$	−2.8	$C_{19}H_{22}$	−2.9	$C_{31}H_{32}$	−2.9
$C_{11}H_{13}$	−2.8	$C_{23}H_{24}$	−2.9	$C_{33}H_{34}$	−2.8
$C_{11}H_{14}$	−2.8	$C_{23}H_{25}$	−2.9	$C_{33}H_{35}$	−2.9
$N_{16}H_{17}$	−2.7	$C_{26}H_{27}$	−2.9		

N_9-H_{10} and O_{29}-H_{30} bonds respectively. Their $V_{s,max}$ reports -2.5×10^3 kJ·mol^{-1} and -2.6×10^3 kJ·mol^{-1} in increasing order. These atoms find the potential HB donor sites. In other words, HB with oryzenin protons is preferably carried out in the order: H_{10} then H_{30}. The following sections discuss the interactions of AM2G-oryzenin complexes.

3.2. Interaction of the AM2G-Oryzenin Complex

Figure 4 illustrate the spatial structure of the complexes after optimization. They show oryzenin interactions with the proton acceptor site of amylose. More, this work discusses the geometrical parameters.

Geometric Parameters

Table 2 shows the geometrical parameters of the AM2G-Oryzenin interaction. These are the distance d (Å), the linearity angles α and directional angle β. The approach distances of HB to the osidic bridge are between 1.88 Å and 2.48 Å. These hydrogen bond lengths are less than 2.62 Å as recommended by [36] and [37]. Generally, the hydrogen bond length between two neutral fragments is about1.5 Å to 2.2 Å [43]. The O_{29}-H_{30}…O_{46} interaction satisfies this constraint. It suggests O_{29}-H_{30}…O_{46} is much stronger than N_9H_{10}…O_{46}. The angle α of O_{29}-H_{30}…O_{46} is the highest (159.8˚). Its relative proximity to 180˚ corroborates the thick interaction O_{29}-H_{30}…O_{46}. The β angle of 102.9˚ confirms this result; it remains close to 90˚. These geometrical features suggest the strength of HB with the osidic bridge is preferentially realized with O_{29}-H_{30}…O_{46}. A greater length than 2.2 Å indicates a weak hydrogen bond. It's with a direction angle that deviates from linearity. This is the case for the N_9-H_{10}…O_{46} interaction. The research also goes interested in the energy parameters.

Energy parameters

Table 3 shows the enthalpies, entropy, and free enthalpies of reaction. These energy parameters aren't revised by the basis set superposition error. The enthalpies indicated that the O_{29}-H_{30}…O_{46} HB appears the most stable. Its enthalpy

Table 2. Geometric parameters of the AM2G-Oryzenin complex at ONIOM (B3LYP/6 - 31 + G (d, p): AM1).

HB with the osidic bridge	d (Å)	α (˚)	β (˚)
O_{29}-H_{30}…O_{46}	1.88	159.8	102.9
N_9-H_{10}…O_{46}	2.48	147.8	108.5

Table 3. Energy parameters of the AM2G-Oryzenin complex at the ONIOM level (B3-LYP/6 - 31 + G (d, p): AM1).

HB with the osidic bridge	$\Delta_r H$ (kcal·mol^{-1})	$\Delta_r S$ (kcal·K^{-1}·mol^{-1})	$\Delta_r G$ (kcal·mol^{-1})
O_{29}-H_{30}…O_{46}	−23.160	−0.044	−10.156
N_9-H_{10}…O_{46}	−8.407	−0.037	2.664

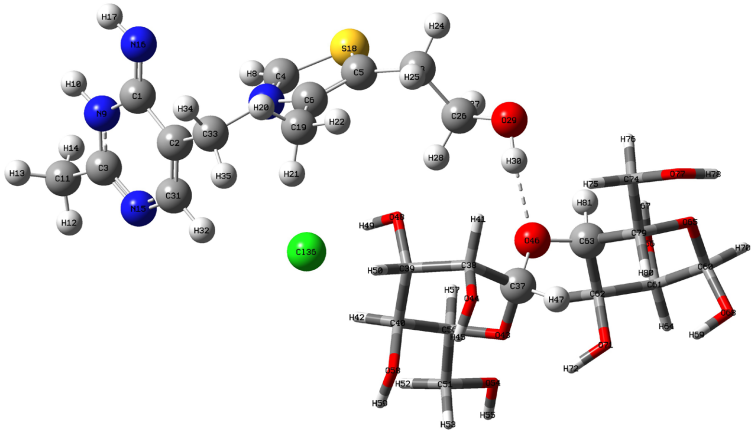

(a)

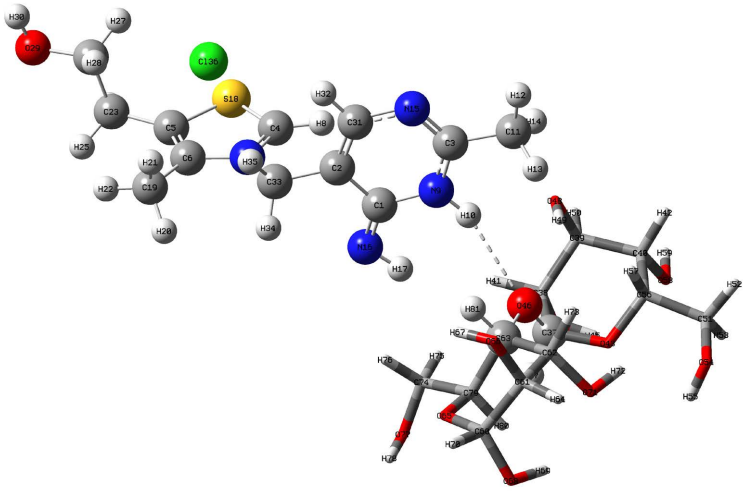

(b)

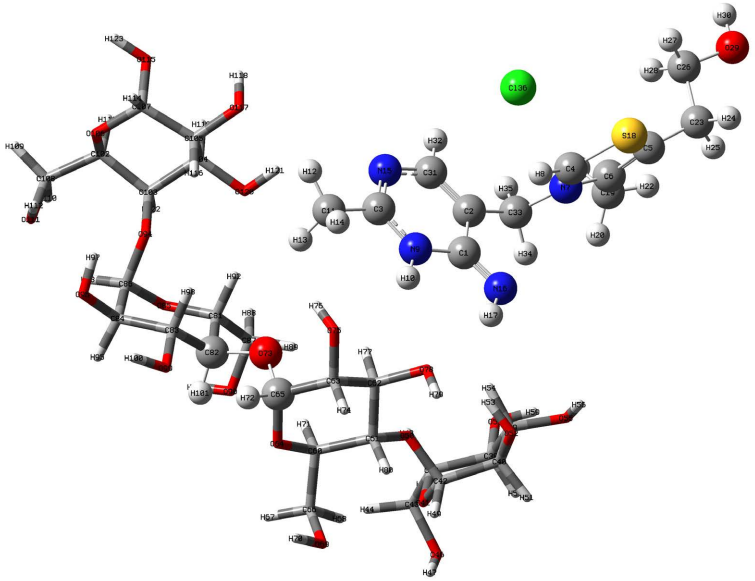

(c)

Figure 4. 3D structures of optimized AM2G-Oryzenin complexes.

(−23.160 kcal·mol^{-1}) is about that of strong HB. It's lower than the HB enthalpies of trichloroacetic acid and triphenylphosphine oxide. These are almost −16 kcal·mol^{-1} [44]. Its free enthalpy of reaction ($\Delta_r G$ = −10.156 kcal·mol^{-1}) proves that this interaction occurs normally; the HB establishment goes spontaneously. The negative value of its entropy reflects the transition from two to a single entity in the gaseous state. They suggest that they not find natural. The N_9-H_{10}…O_{46} interaction is comparable to the hydrogen bond in the phenol-triethylamine interaction (−8.85 kcal·mol^{-1}) [45]. Spectroscopic descriptors can also characterize HB.

Spectroscopic parameters

Table 4 shows the O-H and N-H elongation frequencies of non-complexes and complex oryzenin. $\Delta\upsilon$ indicate their difference. The vibrational frequencies of O-H (3839 cm^{-1}) and N-H (3591 cm^{-1}) of oryzenin are comparable to those calculated for uracil. In principle, their HB are of the same nature. The O-H elongation frequencies of this compound vary from 3901 cm^{-1} to 3882 cm^{-1} while those of N-H are between 3585 cm^{-1} and 3631 cm^{-1}. The O-H stretches of oryzenin differ by 62 cm^{-1} to 43 cm^{-1} from those of uracil. Those of N-H move from −6 cm^{-1} to 40 cm^{-1}. The υ (OH) and υ (NH) of oryzenin are overestimated on average compared to the experimental υ (OH) and υ (NH) of free uracil. These quantities equal 3727 cm^{-1} and 3343 cm^{-1}. The complexation lowers vibrational frequencies. The variation depends on the strength of the HB. The variation of $\Delta\upsilon$ = 232 cm^{-1} in the O_{29}-H_{30}…O_{46} interaction exceeds that of N_9H_{10}…O_{46} ($\Delta\upsilon$ = 65 cm^{-1}). It reflects the relatively strong attraction exerted by the oxygen of the saccharide bridge (O_{46} acceptor) on the hydrogen of the probe. Under these conditions, O_{29}-H_{30}…O_{46} HB becomes stronger than N_9H_{10}…O_{46} one.

For AM2G, the breakdown of amyloidosis takes place mainly through HB O_{29}-H_{30}…O_{46}. In other words, it occurs at the level of the osidic oxygen at the end of the amyloidosis chain. It promotes the presence of monosaccharides in the amylose's degradation products. This research is also interested in the AM3G-oryzenin interaction.

3.3. Interaction of the AM3G-Oryzenin Complex

Figure 5 shows the optimized structures of the AM3G-oryzenin complex. They show the main interactions between these two molecules. This work details their geometrical parameters.

Table 4. Elongation frequency and its variation.

HB AM2G-Oryzenin	Free Oryzenin		Complex Oryzenin		Variations $\Delta\upsilon$	
	O-H	N-H	O-H	N-H	O-H	N-H
O_{29}-H_{30}…O_{46}	3839		3607		232	
N_9-H_{10}…O_{46}		3591		3526		65

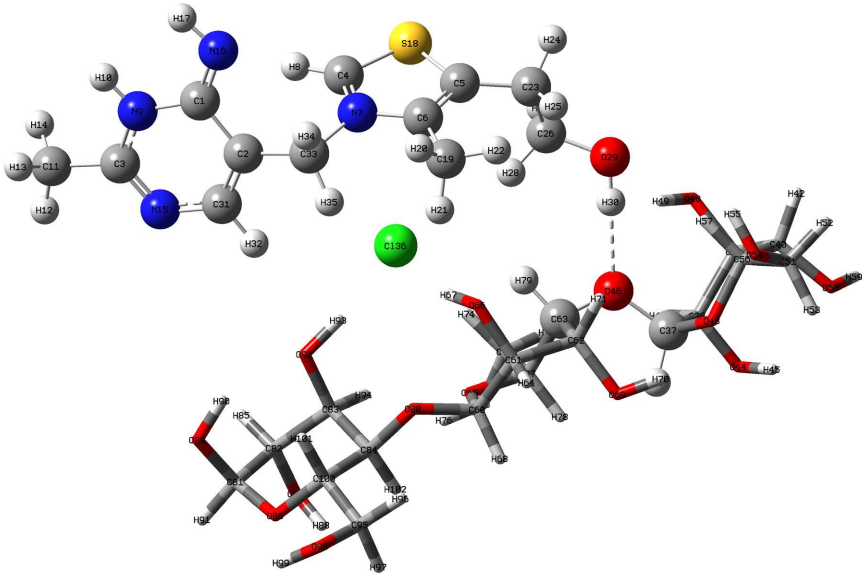

(a)

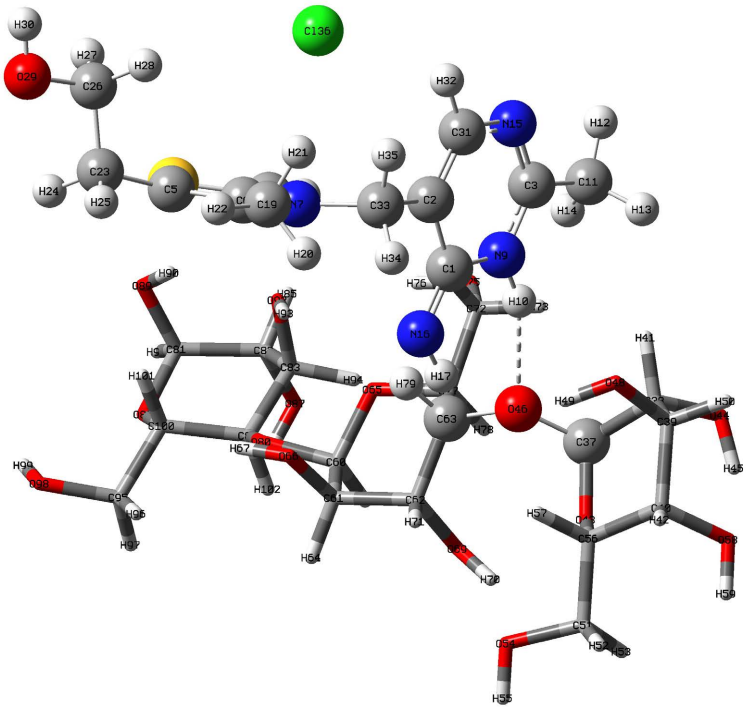

(b)

Figure 5. 3D structures of the optimized AM3G-ORYZENIN complexes.

Geometrical Parameters

The geometric analysis of HB associated with the interaction of AM3G with the oryzenin molecule is based on the recommendations of [37]. **Table 5** shows the HB lengths (d), their linearity (α) and directional angle (β) established with osidic bridge. The HB lengths d of O_{29}-H_{30}…O_{46} and N_9-H_{10}…O_{46} find 1.93 Å and 2.19 Å respectively.

Table 5. Geometrical parameters of the AM3G-Oryzenin complex at the ONIOM level (B3LYP/6 - 31 + G(d, p): AM1).

HB with the osidic bridge	d (Å)	α (˚)	β (˚)
O_{29}-H_{30}…O_{46}	1.93	179.3	102.2
N_9-H_{10}…O_{46}	2.19	161.8	110

They suggest that the first interaction appear the thickest. Moreover, its parameters reveal its stability. The linearity $\alpha = 179.3^\circ$ and the angle $\beta = 102.2^\circ$ sit close to the ideal values ($\alpha = 180^\circ$ and $\beta = 90^\circ$). These parameters indicate that the O_{29}-H_{30}…O_{46} HB reports stronger than those of N_9-H_{10}…O_{46}. The energy factors help to classify the HB of this complex.

Energy parameters

Table 6 shows the enthalpies, entropy, and free enthalpies of reaction O_{29}-H_{30}…O_{46}, and N_9-H_{10}…O_{46}. The first quantities reach $\Delta_r H = -21.037$ kcal·mol^{-1} and $\Delta_r H = -2.309$ kcal·mol^{-1} respectively. These data prove that the O_{29}-H_{30}…O_{46} HB represents more stable of the two. This enthalpy is slightly higher than its correspondent in AM2G. The negative evolution of the free enthalpy during the O_{29}-H_{30}…O_{46} approach ($\Delta_r G = -7.143$ kcal·mol^{-1}) indicates that this is achieved suddenly in contrast to its counterpart ($\Delta_r G = 8.600$ kcal·mol^{-1}). The energy characteristics reflect a stronger interaction of O_{29}-H_{30}…O_{46}. Spectroscopic parameters explain the elongation of HB.

Spectroscopic Parameters

Table 7 shows the elongation frequencies $\upsilon_{(O\text{-}H)}$ and $\upsilon_{(N\text{-}H)}$ of free and complex oryzenin when OH or NH approaches the osidic bridge. Its last column displays the frequency gap. This stands strong for the O_{29}-H_{30}…O_{46} interaction. Its relative value $\Delta\upsilon$ =161 cm^{-1} becomes higher than the second interaction one (N_9-H_{10}…O_{46}: $\Delta\upsilon = 107$ cm^{-1}). The spectroscopic parameters confirm the greater stability of the O_{29}-H_{30}…O_{46} HB. However, this variation in elongation frequency is small compared to that of AM2G. It reflects the fact that the dominant interaction of oryzenin with AM3G is weaker than that with AM2G.

For AM3G, the degradation is mainly related to the formation of HB O_{29}-H_{30}…O_{46}. It involves the atom of the osidic bridge at the end of the AM3G chain. It promotes the presence of monosaccharides in the amylose's degradation products. Moreover, this result indicates that the elongation of a unit doesn't modify the mechanism of its degradation. This research also focuses on the AM4G-oryzenin complex.

3.4. Interaction of the AM4G-Oryzenin Complex

The molecular structure of AM4G has three saccharide bridges. Their interaction with the two HB sites of oryzenin leads to four cases. Figure 6 shows the geometries of the AM4G-oryzenin complex. The osidic oxygen at the end of the chain is called O (1) and that of the middle O (2). The geometric parameters make it possible to identify these interactions.

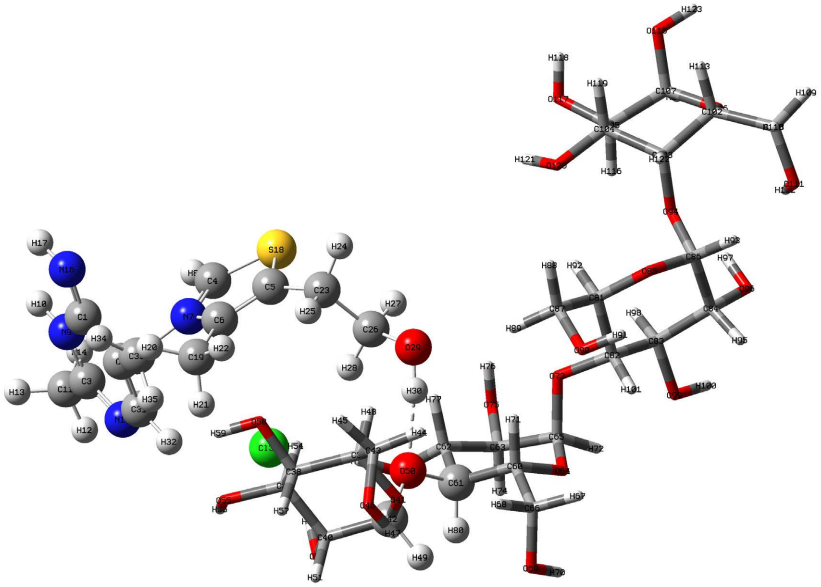

(a)

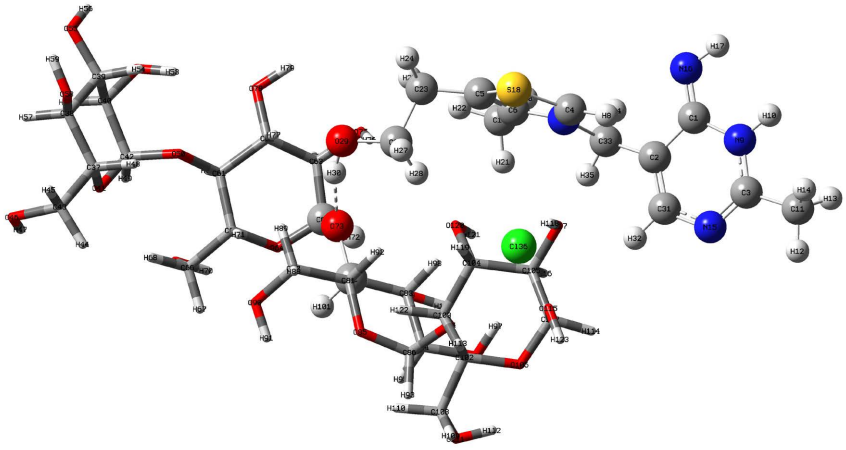

(b)

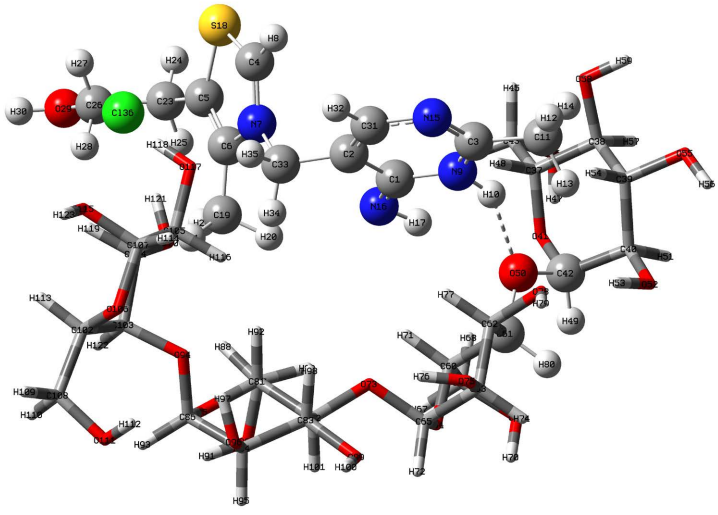

(c)

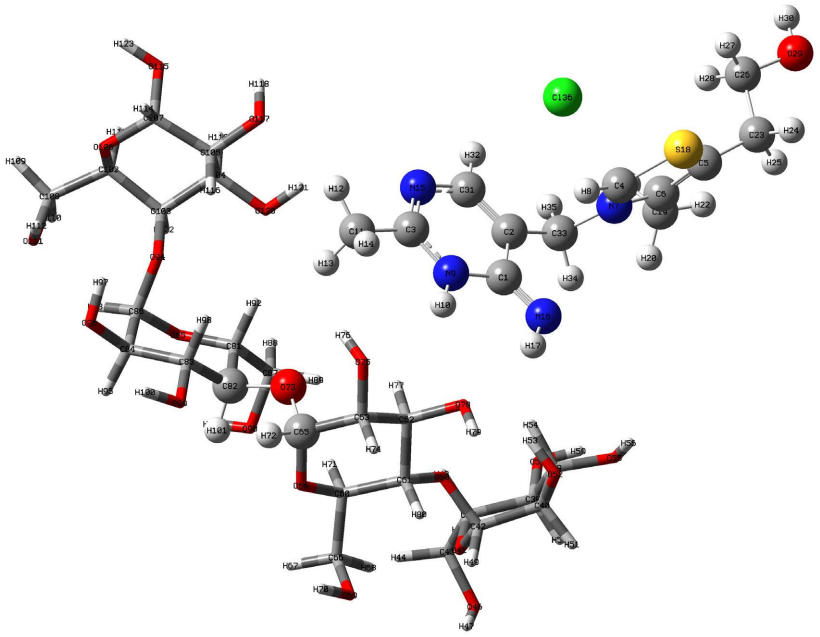

(d)

Figure 6. 3D structures of the optimized AM4G-ORYZENIN complexes.

Table 6. Energy parameters of the AM3G-Oryzenin complex at the ONIOM level (B3-LYP/6 - 31 + G (d, p): AM1).

HB with the osidic bridge	$\Delta_r H$ (kcal·mol^{-1})	$\Delta_r S$ (kcal·K^{-1}·mol^{-1})	$\Delta_r G$ (kcal·mol^{-1})
O_{29}-H_{30}…O_{46}	−21.037	−0.047	−7.143
N_9-H_{10}…O_{46}	−2.309	−0.037	8.600

Table 7. Elongation frequency and variation of elongation frequencies in cm^{-1} of free and complex Oryzenin O-H and N-H in the AM3G-Oryzenin interaction.

HB AM3G-Oryzenin	Free Oryzenin		Complex Oryzenin		Variations $\Delta\upsilon$	
	O-H	N-H	O-H	N-H	O-H	N-H
O_{29}-H_{30}…O_{46}	3839		3678		161	
N_9-H_{10}…O_{46}		3591		3484		107

Geometrical Parameters

The geometry optimization is performed at the DFT/B3LYP/6 - 31 + G(d, p) level of theory. It provides access to the structural features of the AM4G-oryzenin complex.

Table 8 presents its HB lengths (d) and its α linearity and β-directional angles. The strongest HB corresponds to the O_{29}-H_{30}…O (1) interaction. Its HB length (d =1.88 Å) remains the smallest. Its angle α = 164˚ and β = 106.4˚ finds closest to their ideal values. The geometrical parameters indicate that HB O_{29}-H_{30}…O (1) stays the most probable. They provide evidence that under the action of

Table 8. Geometric parameters of the AM4G-Oryzenin complex at the ONIOM level (B3LYP/6 - 31 + G(d, p): AM1).

HB with osidic bridges	d (Å)	α (˚)	β (˚)
O_{29}-H_{30}…O (1)	1.88	164	106.4
O_{29}-H_{30}…O (2)	1.91	160	107.5
N_9-H_{10}…O (1)	2.19	148.9	112.9
N_9-H_{10}…O (2)	4.07	112.1	92.1

oryzenin the degradation of amylose starts at the end of the chain. The distance d = 1.91 Å proves that this process continues in the middle. The products of amylose degradation represent mainly monosaccharides and secondary disaccharides. The latter also deteriorate as AM2G-oryzenin. This result agrees with the observation of [46]. These authors mention that the rice degradation is materialized by a decrease in disaccharides and an increase in monosaccharides. The following section focuses on the energy parameters of these interactions.

Energy Parameters

Table 9 shows the enthalpy, entropy and free enthalpy of reaction variations related to AM4G-oryzenin interaction. The first ($\Delta_r H$ = −35.413 kcal·mol^{-1}) establishes that O_{29}-H_{30}…O (2) HB stands the most stable. Moreover, its formation lives natural; its free enthalpy goes negative ($\Delta_r G$ = −18.291 kcal·mol^{-1}) like other interactions. The entropy varies only slightly.

The energy parameters suggest that this bond appear the most favoured. Otherwise, the dissociation of this amylose starts in the middle of its chain. It continues at its end; the HB (O_{29}-H_{30}…O (1)) is the second most stable ($\Delta_r H$ = −26.410 kcal·mol^{-1}). The spectroscopic parameters allow dealing with this contradiction. In this case, the geometrical and energetic characteristics lead to a controversial conclusion. The former assert that AM4G degradation starts at the end of the chain as a matter of priority, while the latter considers it to be in the middle at the start. Spectroscopic parameters could help to resolve this contradiction.

Spectroscopic parameters

Table 10 contains the elongation frequencies υ(O-H) and υ(N-H) of free and complex oryzenin when the OH or NH hydrogen approaches the osidic bridge. Its last column shows their variations.

There is a decrease in the elongation frequencies of O-H and N-H when oryzenin sits complex. HB leads to an elongation of the O-H and N-H lengths. This represents the effect of charge transfer, which causes a drop in vibrational frequencies.

This decrease is observed in the AM4G-Oryzenin complex. Besides, it's 287 cm^{-1} for the strongest O_{29}-H_{30}…O (1) interaction. This result goes compatible with the one generated by the geometrical parameters. It establishes that this HB predominates for the AM4G-oryzenin complex.

Table 9. Energy parameters in kcal/mol of the AM4G-Oryzenin complex at the ONIOM level (B3LYP/6 - 31 + G (d, p): AM1).

HB with the osidic bridge	$\Delta_r H$ (kcal·mol^{-1})	$\Delta_r S$ (kcal·K^{-1}·mol^{-1})	$\Delta_r G$ (kcal·mol^{-1})
O_{29}-H_{30}…O (1)	−26.410	−0.052	−10.864
O_{29}-H_{30}…O (2)	−35.413	−0.057	−18.291
N_9-H_{10}…O (1)	−14.813	−0.045	−1.278
N_9-H_{10}…O (2)	−15.004	−0.040	−2.944

Table 10. Elongation frequency and variation of elongation frequencies in cm^{-1} of free and complex Oryzenin O-H and N-H in the AM4G-Oryzenin interaction.

HB AM4G-Oryzenin	Free Oryzenin		Complex Oryzenin		Variations Δv	
	O-H	N-H	O-H	N-H	O-H	N-H
O_{29}-H_{30}…O (1)	3839		3552		287	
O_{29}-H_{30}…O (2)	3839		3589		250	
N_9-H_{10}…O (1)		3591		3509		82
N_9-H_{10}…O (2)		3591		3378		213

For AM4G, the degradation is based on the probable formation of O_{29}-H_{30}…O (1). It continues with that of O_{29}-H_{30}…O (2). This result provides evidence that under the action of oryzenin, the alteration of amylose starts at the end of the chain's amylose. It lives secondary to its middle. Besides, the AM2G elongation of two units modifies the mechanism of amylose's transformation. AM4G degrades it at its extremities and its middle. More, NBO analysis offers another way to understand the oryzenin's action of amylose.

3.5. NBO Analysis

Lone pairs of electrons play an important role in chemical processes. NBO analysis provides access to the HB intermolecular energy of X-H…Y type. It proceeds by evaluating the stabilization energy $E^{(2)}$ as illustrated in materials and calculation methods section. Tables 11-13 collect the stabilization energies $E^{(2)}$, the energy differences of NBO electron donors (i) and acceptor one (j) and the Fock matrix elements $F_{i,j}$.

The NBO analysis data show a strong stabilization of the delocalization energy related to the interactions for the single pairs of the chloride ion Cl_{36}. Specifically, the dominant interactions in the complexes report HB linked to the $n^{(4)}_{Cl_{36}} \rightarrow \sigma^*_{O_{48}\text{-}H_{49}}$ transition ($E^{(2)}$ = 35.76 kcal·mol^{-1}), for AM2G-Oryzenin complex, $n^{(4)}_{Cl_{36}} \rightarrow \sigma^*_{O_{92}\text{-}H_{93}}$ ($E^{(2)}$ = 25.58 kcal·mol^{-1}) for AM3G-Oryzenin complex, and $n^{(4)}_{Cl_{36}} \rightarrow \sigma^*_{O_{120}\text{-}H_{121}}$ ($E^{(2)}$ = 33.02 kcal·mol^{-1}) for the AM4G-Oryzenin complex. After these, follow the interactions established with O_{29}-H_{30}. Their

Table 11. Stabilization energy of the second order $E^{(2)}$ perturbations in the AM2G… ORYZENİN complex.

	Transitions	$E^{(2)}$ Kcal/mol	$E(i) - E(j)$ (a.u)	$F(i, j)$ (a.u)	Charge transfer (me)
$O_{29}H_{30}$	$n^{(1)}_{Cl_{36}} \rightarrow \sigma^{*}_{O_{48}\text{-}H_{49}}$	2.30	0.95	0.043	4.10
	$n^{(2)}_{Cl_{36}} \rightarrow \sigma^{*}_{C_{40}\text{-}H_{42}}$	3.07	0.83	0.045	5.88
	$n^{(3)}_{Cl_{36}} \rightarrow \sigma^{*}_{C_{40}\text{-}H_{42}}$	7.70	0.63	0.062	19.37
	$n^{(4)}_{Cl_{36}} \rightarrow \sigma^{*}_{C_{40}\text{-}H_{42}}$	5.81	0.71	0.058	13.35
	$n^{(4)}_{Cl_{36}} \rightarrow \sigma^{*}_{O_{48}\text{-}H_{49}}$	35.76	0.75	0.145	74.76
	$n^{(1)}_{O_{46}} \rightarrow \sigma^{*}_{O_{29}\text{-}H_{30}}$	7.84	1.05	0.081	11.90
	$n^{(2)}_{O_{46}} \rightarrow \sigma^{*}_{O_{29}\text{-}H_{30}}$	4.33	0.82	0.054	8.67
	$n^{(1)}_{O_{48}} \rightarrow \sigma^{*}_{C_{26}\text{-}H_{28}}$	1.60	1.00	0.036	2.59
	$n^{(2)}_{O_{48}} \rightarrow \sigma^{*}_{C_{26}\text{-}H_{28}}$	1.76	0.74	0.032	3.74
$N_9\text{-}H_{10}$	$n^{(1)}_{O_{46}} \rightarrow \sigma^{*}_{N_9\text{-}H_{10}}$	1.60	1.01	0.036	2.54
	$n^{(2)}_{O_{48}} \rightarrow \sigma^{*}_{N_9\text{-}H_{10}}$	2.64	0.77	0.040	5.40

Table 12. Stabilization energy of the second order $E^{(2)}$ perturbations in the AM3G…OR-YZENİN complex.

	Transitions	$E^{(2)}$ Kcal/mol	$E(i) - E(j)$ (a.u)	$F(i, j)$ (a.u)	Charge transfer (me)
$O_{29}H_{30}$	$n^{(1)}_{O_{29}} \rightarrow \sigma^{*}_{O_{48}\text{-}H_{49}}$	1.62	0.80	0.032	3.20
	$n^{(1)}_{Cl_{36}} \rightarrow \sigma^{*}_{O_{92}\text{-}H_{93}}$	2.51	1.14	0.049	3.69
	$n^{(3)}_{Cl_{36}} \rightarrow \sigma^{*}_{O_{66}\text{-}H_{67}}$	12.26	0.68	0.082	29.08
	$n^{(3)}_{Cl_{36}} \rightarrow \sigma^{*}_{O_{92}\text{-}H_{93}}$	7.08	0.69	0.063	16.67
	$n^{(4)}_{Cl_{36}} \rightarrow \sigma^{*}_{O_{66}\text{-}H_{67}}$	19.06	0.81	0.112	38.24
	$n^{(4)}_{Cl_{36}} \rightarrow \sigma^{*}_{O_{92}\text{-}H_{93}}$	25.58	0.82	0.130	50.27
	$n^{(1)}_{O_{46}} \rightarrow \sigma^{*}_{O_{29}\text{-}H_{30}}$	5.20	1.01	0.065	8.28
	$n^{(2)}_{O_{46}} \rightarrow \sigma^{*}_{O_{29}\text{-}H_{30}}$	5.87	0.83	0.063	11.52
	$n^{(2)}_{O_{66}} \rightarrow \sigma^{*}_{C_{19}\text{-}H_{21}}$	2.57	1.01	0.046	4.15
N_9H_{10}	$n^{(1)}_{O_{46}} \rightarrow \sigma^{*}_{N_9\text{-}H_{10}}$	4.62	1.02	0.061	7.15

Table 13. Stabilization energy of the second order $E^{(2)}$ perturbations in the AM4G…ORYZENIN complex.

	Transitions	$E^{(2)}$ Kcal/mol	$E(i) - E(j)$ (a.u)	$F(i, j)$ (a.u)	Charge transfer (me)
$O_{29}H_{30}$…O (1)	$n^{(1)}_{Cl_{36}} \rightarrow \sigma^{*}_{O_{78}\text{-}H_{79}}$	1.86	1.16	0.042	2.62
	$n^{(2)}_{Cl_{36}} \rightarrow \sigma^{*}_{C_{39}\text{-}H_{54}}$	2.97	0.67	0.040	7.13
	$n^{(3)}_{Cl_{36}} \rightarrow \sigma^{*}_{O_{52}\text{-}H_{53}}$	5.55	0.71	0.056	12.44
	$n^{(3)}_{Cl_{36}} \rightarrow \sigma^{*}_{O_{55}\text{-}H_{56}}$	2.94	0.73	0.042	6.62
	$n^{(3)}_{Cl_{36}} \rightarrow \sigma^{*}_{O_{78}\text{-}H_{79}}$	4.91	0.73	0.053	10.54
	$n^{(4)}_{Cl_{36}} \rightarrow \sigma^{*}_{O_{52}\text{-}H_{53}}$	19.76	0.79	0.113	40.92
	$n^{(4)}_{Cl_{36}} \rightarrow \sigma^{*}_{O_{78}\text{-}H_{79}}$	15.90	0.81	0.102	31.71
	$n^{(1)}_{O(1)} \rightarrow \sigma^{*}_{O_{29}\text{-}H_{30}}$	5.43	0.99	0.066	8.89
	$n^{(2)}_{O(1)} \rightarrow \sigma^{*}_{O_{29}\text{-}H_{30}}$	9.32	0.84	0.080	18.14
	$n^{(2)}_{O_{55}} \rightarrow \sigma^{*}_{O_{29}\text{-}H_{30}}$	3.18	0.75	0.044	6.88
$O_{29}H_{30}$…O (2)	$n^{(1)}_{O_{29}} \rightarrow \sigma^{*}_{O_{120}\text{-}H_{121}}$	3.27	1.05	0.052	4.91
	$n^{(2)}_{O_{29}} \rightarrow \sigma^{*}_{O_{120}\text{-}H_{121}}$	3.12	0.85	0.046	5.86
	$n^{(1)}_{O(2)} \rightarrow \sigma^{*}_{O_{29}\text{-}H_{30}}$	2.80	1.04	0.048	4.26
	$n^{(2)}_{O(2)} \rightarrow \sigma^{*}_{O_{29}\text{-}H_{30}}$	6.34	0.82	0.065	12.57
N_9H_{10}…O (1)	$n^{(1)}_{Cl_{36}} \rightarrow \sigma^{*}_{O_{117}\text{-}H_{118}}$	1.56	1.12	0.038	2.30
	$n^{(1)}_{Cl_{36}} \rightarrow \sigma^{*}_{O_{120}\text{-}H_{121}}$	2.58	1.10	0.049	3.97
	$n^{(3)}_{Cl_{36}} \rightarrow \sigma^{*}_{O_{117}\text{-}H_{118}}$	16.11	0.68	0.094	38.22
	$n^{(3)}_{Cl_{36}} \rightarrow \sigma^{*}_{O_{120}\text{-}H_{121}}$	1.92	0.65	0.032	4.85
	$n^{(4)}_{Cl_{36}} \rightarrow \sigma^{*}_{O_{120}\text{-}H_{121}}$	33.02	0.76	0.142	69.82
	$n^{(1)}_{O(1)} \rightarrow \sigma^{*}_{N_9\text{-}H_{10}}$	4.40	1.03	0.063	7.48
	$n^{(1)}_{O_{78}} \rightarrow \sigma^{*}_{C_{11}\text{-}H_{13}}$	1.57	1.04	0.036	2.40
	$n^{(2)}_{O_{117}} \rightarrow \sigma^{*}_{C_{33}\text{-}H_{35}}$	3.46	0.73	0.045	7.60
N_9H_{10}…O (2)	$n^{(1)}_{O_{78}} \rightarrow \sigma^{*}_{N_{16}\text{-}H_{17}}$	3.51	1.14	0.057	5.00

stabilization energies correspond to 7.84 kcal·mol^{-1} for the $n^{(1)}_{O_{46}} \rightarrow \sigma^{*}_{O_{29}\text{-}H_{30}}$ transition in AM2G-Oryzenin complex, 5.87 kcal·mol^{-1} in AM3G-Oryzenin complex and 9.32 kcal·mol^{-1} for the AM4G-Oryzenin complex.

The NBO analysis corroborates that the main HB of the amylose-oryzenin complexes results from the interaction between O_{29}-H_{30} and the oxygen of the osidic bridge. Furthermore, for AM4G-oryzenin complex, the strongest HB is established with this latter at the end of the chain. This result confirms that the products of amylose degradation find predominately monosaccharides; it substantiates the experimental observation of [46]. This last discussion leads us to conclude this work.

4. Conclusions

Rice, which has 90% starch, tends to degrade during storage. Efficient processes limit post-harvest losses; these are related to external factors such as humidity, temperature, fungi, such as. Internal causes contribute to it; oryzenin alters its amyloidosis. Chemistry misunderstood its mechanism. Its theoretical aspect offers a way to explore it.

This work exploits the quantum computing resources of the ONIOM strategy (DFT/B3LYP/6 - 31 + G(d, p): AM1) in this viewpoint. It demonstrates that oryzenin associates with amyloidosis through a strong HB. The latter is preferably established between an oryzenin's hydroxyl group and the osidic bridge's oxygen of the amylose. This atom is at the end of the chain.

This mechanism accounts for the abundance of monosaccharides observed in the starch's degradation products. It also explains the occasional presence of disaccharides in these products; oryzenin begins to act on the oxygen in the osidic bridge in the middle of the chain. This reactive attack pattern promotes the presence of disaccharides in the rice starch's degradation products. More, knowledge amylose's degradation mechanism by oryzenin provides a first avenue for listing the molecular processes likely to hinder it in hybrid rice. The latter can be stockpiled longer than its counterparts. It leads to reduced post-harvest losses. For [3], this variety is becoming a lever in the fight against poverty in poor countries; stored rice surpluses fuel the creation of jobs in milling, marketing, or trading. Besides, this exploratory research provides a partial understanding of the oryzenin action on starch. This also contains amylopectin; its reaction with oryzenin represents the team's next work. More, ESP favours the N_9-H_{10} site over O_{29}-H_{30} while the data relating to intermolecular interactions prefer the latter. This apparent contradiction can be explained by the small difference in their potential energies; these are equal to (-2.6×10^3 kJ mol^{-1}) for O_{29}-H_{30} and (-2.5×10^3 kJ mol^{-1}) for N_9-H_{10}.

Conflicts of Interest

The authors declare no conflict of interest regarding the publication of this paper.

References

[1] Bamba, E.H.S. (2016) En route pour la pérénnisation des cantines scolaires. Direction des cantines scolaires, Abidjan.

[2] Dabat, M.-H., Treyer, O.J., Razafimandimby, S. and Bockel, L. (2008) L'histoire inachevée de la régulation du marché du riz à Madagascar. *Économie Rurale*, **303-304-305**, 75-89.

[3] Salle de presse (2008) Le riz: Les enjeux en question. https://www.fao.org/Newsroom/fr/focus/2004/36887/article_36967fr.html

[4] Cruz, J.-F., Hounhouigan, D.J. and Fleurat-Lessard, F. (2016) La conservation des grains après récolte. Presses agronomiques de Gembloux, Gembloux. https://doi.org/10.35690/978-2-7592-2437-1

[5] Pardey, P., Koo, B. and Nottenburg, C. (2003) Création, Protection et utilisation des biotechnologies agricoles dans le monde à l'ère de la propriété intellectuelle. *WIPO-UPOV Symposium on Intellectual Property Rights in Plant Biotechnology*, Genève.

[6] Juliano, B.O. (1985) Polysaccharides, Protein, and Lipids of Rice. *Rice Chemistry and Technology*, American Association of Cereal Chemist, Saint Paul, 59-174.

[7] Park, C.-E., Kim, Y.-S., Park, K.-J. and Kim, B.-K. (2012) Changes in Physicochemical Characteristics of Rice during Storage at Different Temperatures. *Journal of Stored Products Research*, **48**, 25-29. https://doi.org/10.1016/j.jspr.2011.08.005

[8] Diawara, B. (1988) Conservation de riz-paddy sous atmosphères controlées : aspects microbiologiques et conséquences technologiques. Thèse de doctorat, Université de Nantes.

[9] Aidoo, K.E. (1993) Post-Harvest Storage and Preservation of Tropical Crops. *International Biodeterioration & Biodegradation*, **32**, 161-173. https://doi.org/10.1016/0964-8305(93)90048-7

[10] Sholberg, P.L. (1996) Fumigation of High Moisture Seed with Acetic Acid to Control Storage Mold. *Canadian Journal of Plant Science*, **76**, 551-555. https://doi.org/10.4141/cjps96-100

[11] Buckman, K.A., Campbell, J.F. and Subramanyam, B. (2013) *Tribolium castaneum* (Coleoptera: Tenebrionidae) Associated with Rice Mills: Fumigation Efficacy and Population Rebound. *Journal of Economic Entomology*, **106**, 499-512. https://doi.org/10.1603/EC12276

[12] Pacaud, G. (1998) Aperçu sur la désinsectisation par anoxie sous atmosphère inerte. 1. Systèmes statique et dynamique (1). *La lettre de l'OCIM*, No. 58, 26-30.

[13] Bason, M.L., Gras, P.W., Banks, H.J. and Esteves, L.A. (1990) A Quantitative Study of the Influence of Temperature, Water Activity and Storage Atmosphere on the Yellowing of Paddy Endosperm. *Journal of Cereal Science*, **12**, 193-201. https://doi.org/10.1016/S0733-5210(09)80101-X

[14] Chrastil, J. (1990) Protein-Starch Interactions in Rice Grains. Influence of Storage on Oryzenin and Starch. *Journal of Agricultural and Food Chemistry*, **38**, 1804-1809. https://doi.org/10.1021/jf00099a005

[15] Wongdechsarekul, S. and Kongkiattikajorn, J. (2010) Storage Time Affects Storage Proteins and Volatile Compounds, and Pasting Behavior of Milled Rice. *KKU Research Journal*, **15**, 852-862.

[16] Cipcigan, F., Sokhan, V., Martyna, G. and Crain, J. (2018) Structure and Hydrogen Bonding at the Limits of Liquid Water Stability. *Scientific Reports*, **8**, Article No. 1718. https://doi.org/10.1038/s41598-017-18975-7

[17] Liu, J., He, X., Zhang, J.Z.H. and Qi, L.-W. (2018) Hydrogen-Bond Structure Dynamics in Bulk Water: Insights from *ab Initio* Simulations with Coupled Cluster Theory. *Chemical Science*, **9**, 2065-2073. https://doi.org/10.1039/C7SC04205A

[18] Gilli, P., Bertolasi, V., Pretto, L., Ferretti, V. and Gilli, G. (2004) Covalent versus Electrostatic Nature of the Strong Hydrogen Bond: Discrimination among Single, Double, and Asymmetric Single-Well Hydrogen Bonds by Variable-Temperature X-ray Crystallographic M. *Journal of the Ameican Chemical Society*, **126**, 3845-3855. https://doi.org/10.1021/ja030213z

[19] Gilli, P., Bertolasi, V., Pretto, L., Ferretti, V. and Gilli, G. (1994) Evidence for Resonance-Assisted Hydrogen Bonding. Covalent Nature of the Strong Homonuclear Hydrogen Bond. Study of the O-H-O System by Crystal Structure Correlation Methods. *Jounal of Americam Society*, **116**, 909-915. https://doi.org/10.1021/ja00082a011

[20] Gilli, P., Bertolasi, V., Pretto, L., Ferretti, V. and Gilli, G. (2000) Evidence for Intramolecular N−H···O Resonance-Assisted Hydrogen Bonding in β-Enaminones and Related Heterodienes. A Combined Crystal-Structural, IR and NMR Spectroscopic, and Quantum-Mechanical. *Journal of the American Society*, **122**, 10405-10417. https://doi.org/10.1021/ja000921+

[21] Behzadi, H., Esrafili, M.D. and Hadipour, N.L. (2007) A Theoretical Study of ^{17}O, ^{14}N and ^{2}H Nuclear Quadrupole Coupling Tensors in the Real Crystalline Structure of Acetaminophen. *Chemical Physics*, **333**, 97-104. https://doi.org/10.1016/j.chemphys.2007.01.011

[22] Esrafili, M.D., Behzadi, H. and Hadipour, N.L. (2008) ^{14}N and ^{17}O Electric Field Gradient Tensors in Benzamide Clusters: Theoretical Evidence for Cooperative and Electronic Delocalization Effects in N−H···O Hydrogen Bonding. *Chemical Physics*, **348**, 175-180. https://doi.org/10.1016/j.chemphys.2008.02.056

[23] Reed, A.E., Curtiss, L.A. and Weinhold, F. (1988) Intermolecular Interactions from a Natural Bond Orbital, Donor-Acceptor Viewpoint. *Chemical Reviews*, **88**, 899-926. https://doi.org/10.1021/cr00088a005

[24] Weinhold, F. (2012) Natural Bond Orbital Analysis: A Critical Overview of Relationships to Alternative Bonding Perspectives. *Journal of Computational Chemistry*, **33**, 2363-2379. https://doi.org/10.1002/jcc.23060

[25] Dapprich, S., Komáromi, I., Byun, K.S., Morokuma, K. and Frisch, M.J. (1999) A new ONIOM Implementation in Gaussian98. Part I. The Calculation of Energies, Gradients, Vibrational Frequencies and Electric Field Derivatives 1 Dedicated to Professor Keiji Morokuma in Celebration of His 65th Birthday.1. *Journal of Molecular Structure*: *THEOCHEM*, **461-462**, 1-21. https://doi.org/10.1016/S0166-1280(98)00475-8

[26] Vreven, T., Byun, K.S., Komáromi, I., Dapprich, S., Montgomery, J.A., Morokuma, K. and Frisch, M.J. (2006) Combining Quantum Mechanics Methods with Molecular Mechanics Methods in ONIOM. *Journal of Chemical Theory and Computation*, **2**, 815-826. https://doi.org/10.1021/ct050289g

[27] Frisch, M.J., Trucks, G.W., Schlegel, H.B., Scuseria, G.E., Robb, M.A., Cheeseman, J.R., Scalmani, G., Baronne, V., Mennucci, B., Peterson, G.A., Nakatsuji, H., Caricato, M., Li, X., Hratchian, H.P., Izmaylov, A.F., Bloino, J., Zheng, G. and Sonnenberg, J.L. (2009) Gaussian 09, Revision A.02. Gaussian, inc., Wallingford.

[28] Günay, N., Pir, H., Avcı, D. and Atalay, Y. (2013) NLO and NBO Analysis of Sarcosine-Maleic Acid by Using HF and B3LYP Calculations. *Journal of Chemistry*, **2013**, Article ID: 712130. https://doi.org/10.1155/2013/712130

[29] Murray, J.S. and Sen, K. (1996) Molecular Electrostatic Potentials: Concepts and

Applications. Elsevier, Amsterdam, 105-538.

[30] Brinck, T. (1998) The Use of the Electrostatic Potential for Analysis and Prediction of Intermolecular Interactions. *Theoretical and Computational Chemistry*, **5**, 51-93. https://doi.org/10.1016/S1380-7323(98)80005-8

[31] Demircioğlu, Z., Albayrak, Ç. and Büyükgüngör, O. (2014) Theoretical and Experimental Investigation of (E)-2-([3,4-dimethylphenyl)imino]methyl)-3-methoxyphenol: Enol-keto Tautomerism, Spectroscopic Properties, NLO, NBO and NPA Analysis. *Journal of Molecular Structure*, **1065**-**1066**, 210-222. https://doi.org/10.1016/j.molstruc.2014.02.062

[32] Bader, R.F.W., Carroll, M.T., Cheeseman, J.R. and Chang, C. (1987) Properties of Atoms in Molecules: Atomic Volumes. *Journal of the American Chemical Society*, **109**, 7968-7979. https://doi.org/10.1021/ja00260a006

[33] Arunan, E., Desiraju, G.R., Klein, R.A., Sadlej, J., Scheiner, S., Alkorta, I., Clary, D.C., Crabtree, R.H. and Dannenberg, J.J. (2011) Definition of the Hydrogen Bond (IUPAC Recommendations 2011). *Pure and Applied Chemistry*, **83**, 1637-1641. https://doi.org/10.1351/PAC-REC-10-01-02

[34] Rowland, R.S. and Taylor, R. (1996) Intermolecular Nonbonded Contact Distances in Organic Crystal Structures: Comparison with Distances Expected from van der Waals Radii. *The Journal of Physical Chemistry*, **100**, 7384-7391. https://doi.org/10.1021/jp953141+

[35] Bondi, A. (1954) Van der Waals Volumes and Radii. *The Journal of Physical Chemistry*, **68**, 441-451. https://doi.org/10.1021/j100785a001

[36] Jorly, J. and Eluvathinga, J.D. (2007) Red-, Blue-, or No-Shift in Hydrogen Bonds: A Unified Explanation. *Journal of the American Chemical Society*, **129**, 4620-4632. https://doi.org/10.1021/ja067545z

[37] Desiraju, G. and Steiner, T. (2001) The Weak Hydrogen Bond: In Structural Chemistry and Biology. Oxford University Press, Oxford, 480. https://doi.org/10.1093/acprof:oso/9780198509707.001.0001

[38] Alabugin, I.V., Manoharan, M., Peabody, S. and Weinhold, F. (2003) Electronic Basis of Improper Hydrogen Bonding: A Subtle Balance of Hyperconjugation and Rehybridization. *Journal of the American Chemical Society*, **125**, 5973-5987. https://doi.org/10.1021/ja034656e

[39] Murray, J.S., Concha, M.C., Lane, P., Hobza, P. and Politzer, P. (2008) Blue Shifts vs Red Shifts in σ-Hole Bonding. *Journal of Molecular Modeling*, **14**, 699-704. https://doi.org/10.1007/s00894-008-0307-y

[40] Chocholoušová, J., Špirko, V. and Hobza, P. (2004) First Local Minimum of the Formic Acid Dimer Exhibits Simultaneously Red-Shifted O–H···O and Improper Blue-Shifted C–H···O Hydrogen Bonds. *Physical Chemistry Chemical Physics*, **6**, 37-41. https://doi.org/10.1039/B314148A

[41] Snehalatha, M., Ravikumar, C., Hubert Joe, I., Sekar, N. and Jayakumar, V.S. (2009) Spectroscopic Analysis and DFT Calculations of a Food Additive Carmoisine. *Spectrochimica Acta Part A: Molecular and Biomolecular Spectroscopy*, **72**, 654-662. https://doi.org/10.1016/j.saa.2008.11.017

[42] Kouassi, A.K., Koné, S. and Bamba, E.H.S. (2021) Water and Dioxide Carbon Effects on Di or Tri Saccharides Degradation by Density Functional Theory at Level: B3LYP/6-311++G(d, p). *Journal of Materials Physics and Chemistry*, **9**, 1-8.

[43] Jeffrey, G.A. (1997) An Introduction to Hydrogen Bonding. Oxford University Press, Oxford.

[44] Hadži, D. and Rajnvajn, J. (1973) Hydrogen Bonding in Some Adducts of Oxygen Bases with Acids. Part 7: Thermodynamic Study by Infra-Red Spectroscopy of the Association of Chloroacetic Acids with Some Oxygen Bases. *Journal of the Chemical Society, Faraday Transactions* 1, **69**, 151-155. https://doi.org/10.1039/f19736900151

[45] Kogowskl, G., Scott, R.M. and Flllsko, F. (1980) Enthalpy Change of Hydrogen Bond Formation between Ortho-Substituted Phenols and Aliphatic Amines. *Journal of Physical Chemistry*, **84**, 2262-2265. https://doi.org/10.1021/j100455a009

[46] Cao, Y., Wang, Y., Chen, X. and Ye, J. (2004) Study on Sugar Profile of Rice during Ageing by Capillary Electrophoresis with Electrochemical Detection. *Food Chemistry*, **86**, 131-136. https://doi.org/10.1016/j.foodchem.2003.12.004